Operating diagram of a flocculation model in the chemostat

R. Fekih-Salem, Tewfik Sari

Operating diagram of a flocculation model in the chemostat

R. Fekih-Salem [a,c,*] — T. Sari [b]

[a] LAMSIN (LR-99-ES20), ENIT, Université de Tunis El Manar
B.P. 37, Le Belvédère, 1002 Tunis, Tunisie
(E-mail: radhouene.fekihsalem@isima.rnu.tn)

[b] ITAP, Univ Montpellier, Irstea, Montpellier SupAgro, Montpellier, France
(E-mail: tewfik.sari@irstea.fr)

[c] ISIMa, Université de Monastir
BP 49, Cité universitaire, 5111 Mahdia, Tunisie.

[*] Corresponding author.

ABSTRACT. The objective of this study is to analyze a model of the chemostat involving the attachment and detachment dynamics of planktonic and aggregated biomass in the presence of a single resource. Considering the mortality of species, we give a complete analysis for the existence and local stability of all steady states for general monotonic growth rates. The model exhibits a rich set of behaviors with a multiplicity of coexistence steady states, bi-stability, and occurrence of stable limit cycles. Moreover, we determine the operating diagram which depicts the asymptotic behavior of the system with respect to control parameters. It shows the emergence of a bi-stability region through a saddle-node bifurcation and the occurrence of coexistence region through a transcritical bifurcation. Finally, we illustrate the importance of the mortality on the destabilization of the microbial ecosystem by promoting the washout of species.

RÉSUMÉ. L'objectif de cette étude est d'analyser un modèle du chémostat impliquant la dynamique d'attachement et de détachement de la biomasse planctonique et agrégée en présence d'une seule ressource. En considérant la mortalité des espèces, nous donnons une analyse complète de l'existence et de la stabilité locale de tous les équilibres pour des taux de croissance monotones. Le modèle présente un ensemble riche de comportements avec multiplicité d'équilibres de coexistence, bi-stabilité et apparition des cycles limites stables. De plus, nous déterminons le diagramme opératoire qui décrit le comportement asymptotique du système par rapport aux paramètres de contrôle. Il montre l'émergence d'une région de bi-stabilité via une bifurcation nœud col et l'occurrence d'une région de coexistence via une bifurcation transcritique. Enfin, nous illustrons l'importance de la mortalité sur la déstabilisation de l'écosystème microbien en favorisant le lessivage des espèces.

KEYWORDS : Bi-stability, Bifurcation, Chemostat, Flocculation, Operating diagram

MOTS-CLÉS : Bi-stabilité, Bifurcation, Chémostat, Floculation, Diagramme opératoire

1. Introduction

In the culture of microorganisms, the processes of attachment and detachment of bacteria are well known and frequently observed. This phenomenon is manifested either by fixation of microorganisms on support as in the growth of biofilms or simply by an aggregation such as the formation of flocs or granules [10, 16]. In fact, the formation of flocs has a direct impact on growth dynamics, since the access to the substrate is limited for microorganisms within such structures. Nevertheless, it is only recently that they have been explicitly taken into account in mathematical models based on the chemostat (see the monograph [8]).

This flocculation mechanism may explain the coexistence of microbial species when the most competitive species inhibits its own growth by the formation of flocs [9]. In fact, these bacteria in flocs consume less substrate than planktonic bacteria since the attached bacteria have less access to the substrate, given that this access to the substrate is proportional to the outside surface of flocs. An extension of the model [9] has been studied in [5] when the growth rate of isolated bacteria of the most competitive species exhibits an inhibition. In this case, there may be coexistence around a stable limit cycle. The interested reader can refer to [4, 5] for a review of the different specific attachment and detachment rates used in the literature.

In this work, we consider the flocculation model of one species introduced in [4]. This model, which has been studied also in [3, 8, 12, 13], is written as follows:

$$\left\{\begin{array}{lcl} \dot{S} & = & D(S_{in}-S)-f(S)u-g(S)v \\ \dot{u} & = & [f(S)-D_u]u-a(u+v)u+bv \\ \dot{v} & = & [g(S)-D_v]v+a(u+v)u-bv \end{array}\right. \tag{1}$$

where $S(t)$ is the concentration of the substrate at time t; $u(t)$ and $v(t)$ are, respectively, the concentrations of planktonic and attached bacteria at time t; $f(S)$ and $g(S)$ represent, respectively, the growth rates of isolated and attached bacteria; D and S_{in} are, respectively, the dilution rate and the concentration of the substrate in the feed device; D_u and D_v represent, respectively, the disappearance rates of planktonic and attached bacteria.

We assume that isolated bacteria can aggregate with isolated bacteria or flocs to form new flocs with a rate $a(u+v)u$, where a is a positive constant, proportional to both the density of isolated bacteria u and the total biomass density $u+v$. Furthermore, the flocs can split and liberate isolated bacteria with rate bv, where b is a positive constant, proportional to their density v.

The study of this model (1) has been limited to the biologically interesting case $D_v \leq D_u \leq D$, where $D_u = \alpha D$ and $D_v = \beta D$, α and β belong to $[0,1]$ and represent, respectively, the fraction of planktonic and attached bacteria leaving the reactor. The factor α was introduced in [2], see also [1], to model a reactor with biomass attached to the support or to decouple the residence time of solids and the hydraulic residence time $(1/D)$.

In this work, we study the model (1) where D_u and D_v can be modeled as in [11, 14] by:

$$D_u = \alpha D + m_u, \quad D_v = \beta D + m_v$$

where the non-negative parameters m_u and m_v representing mortality (or maintenance) rate are taken into consideration. Therefore, our study will not be restricted to the cases $D_v \leq D_u \leq D$, as in [3, 4, 8, 12, 13], and the cases $D < D_u$, $D < D_v$ or $D_u < D_v$, which are also of biological interest, will be investigated.

For the complete mathematical analysis of model (1), the reader is referred to [6]. Our main objective in this paper is to describe the operating diagram of the model in order to illustrate the behavior of the system according to the control parameters D and S_{in}.

This paper is organized as follows. First, we present in Section 2 some general hypotheses about the growth functions of flocculation model (1). Then, we analyze the existence and the local stability of steady states according to the dilution rate and the disappearance rates of planktonic and attached bacteria. In Section 3, we present the operating diagram in order to show the regions of emergence of multiplicity of positive steady states according to the control parameters. In Section 4, we study the one-parameter bifurcation diagrams and the numerical simulations in order to validate the theoretical analysis of the operating diagram. Finally, conclusions are drawn in the last Section 5.

2. Hypotheses and model analysis

We use the following general hypotheses for growth functions $f(S)$ and $g(S)$:

(H1) $f(0) = g(0) = 0$ and $f'(S) > 0$ and $g'(S) > 0$ for all $S > 0$.

(H2) $f(S) > g(S)$ for all $S > 0$.

Assumption (H1) means that the growth can take place if and only if the substrate is present. In addition, the growth rates of isolated and attached bacteria increase with the concentration of substrate. Assumption (H2) means that bacteria in flocs consume less substrate than isolated bacteria.

The following result shows that our model (1) preserves the biological meaning.

Proposition 2.1 *For any non-negative initial condition, the solutions of system (1) remain non-negative and positively bounded. In addition, the set*

$$\Omega = \left\{ (S,u,v) \in \mathbb{R}^3_+ : S + u + v \leq \frac{D}{D_{\min}} S_{in} \right\}, \quad \textit{where} \quad D_{\min} = \min(D, D_u, D_v),$$

is positively invariant and is a global attractor for the dynamics (1).

The proofs of all results of this section are detailed in [6]. In the following, we use the following notations:

$$\varphi(S) = f(S) - D_u \quad \text{and} \quad \psi(S) = g(S) - D_v,$$

$$U(S) := \frac{\varphi(S)\,(\psi(S) - b)}{a\,[\psi(S) - \varphi(S)]} \quad \text{and} \quad V(S) := -\frac{\varphi^2(S)\,(\psi(S) - b)}{a\,[\psi(S) - \varphi(S)]\,\psi(S)}, \tag{2}$$

$$H(S) := f(S)U(S) + g(S)V(S). \tag{3}$$

From (H1), when equations $f(S) = D_u$, $g(S) = D_v$ and $\psi(S) = b$ have solutions, they are unique and we define the usual *break-even concentrations*

$$\lambda_u = f^{-1}(D_u), \quad \lambda_v = g^{-1}(D_v) \quad \text{and} \quad \lambda_b = \psi^{-1}(b).$$

From (H2), if in addition $D_v \geq D_u$, then $\lambda_v > \lambda_u$. When equations $f(S) = D_u$ or $g(S) = D_v$ or $\psi(S) = b$ have no solution, we put $\lambda_u = \infty$ or $\lambda_v = \infty$ or $\lambda_b = \infty$.

2.1. Existence of steady states

In order to study the existence of steady states of model (1), we define the interval I by:

$$I = \begin{cases}]\lambda_u, \lambda_v[& \text{if} \quad \lambda_u < \lambda_v \\ ]\lambda_v, \min(\lambda_u, \lambda_b)[& \text{if} \quad \lambda_u > \lambda_v. \end{cases} \tag{4}$$

We can state the following result:

Lemme 2.1 *Under the assumptions (H1-H2), system (1) has the following steady states:*

1) the washout $E_0 = (S_{in}, 0, 0)$, that always exists,

2) a positive steady state, $E_1 = (S^*, u^*, v^*)$ with S^* solution of equation

$$D(S_{in} - S^*) = H(S^*)$$

where H is given by (3), $u^* = U(S^*)$ and $v^* = V(S^*)$, where U and V are given by (2). This coexistence steady state exists if and only if $S^* \in I$ where I is defined by (4).

The following proposition presents the number of positive steady states of (1).

Proposition 2.2

– When $D_u \leq D_v$, then the positive steady state $E_1 = (S^*, u^*, v^*)$ exists if and only if $S_{in} > \lambda_u$. If it exists, it is unique.

– When $D_u > D_v$, then there exists at least one positive steady state in the case $\lambda_u < \min(\lambda_v, S_{in})$ or $\lambda_v < \min(\lambda_u, \lambda_b) < S_{in}$. Generically, the system can have generically an odd number of positive steady states. When $S_{in} < \min(\lambda_u, \lambda_b)$ and $\lambda_v < \lambda_u$, then generically the system has no positive steady state or an even number of positive steady states.

2.2. Stability of steady states

In this section, we study the local asymptotic stability of each steady state of system (1). Let J be the Jacobian matrix of (1) at (S, u, v), that is given by

$$J = \begin{bmatrix} -D - f'(S)u - g'(S)v & -f(S) & -g(S) \\ f'(S)u & \varphi(S) - a(2u + v) & -au + b \\ g'(S)v & a(2u + v) & \psi(S) + au - b \end{bmatrix}.$$

The stability of the washout steady state is given as follows:

Proposition 2.3 *E_0 is Locally Exponentially Stable (LES) if and only if $S_{in} < \lambda_u$ and $S_{in} < \lambda_b$.*

In the following, we analyze the stability of positive steady states. At $E_1 = (S^*, u^*, v^*)$, the Jacobian matrix is given by

$$J_1 = \begin{bmatrix} -m_{11} & -m_{12} & -m_{13} \\ m_{21} & -m_{22} & a_{23} \\ m_{31} & m_{32} & -m_{33} \end{bmatrix}$$

where

$$\begin{cases} m_{11} = D + f'(S^*)u^* + g'(S^*)v^*, \quad m_{12} = f(S^*), \quad m_{13} = g(S^*), \\ m_{21} = f'(S^*)u^*, \quad m_{22} = a(2u^* + v^*) - \varphi(S^*), \quad a_{23} = b - au^*, \\ m_{31} = g'(S^*)v^*, \quad m_{32} = a(2u^* + v^*) \quad \text{and} \quad m_{33} = b - au^* - \psi(S^*). \end{cases}$$

The characteristic polynomial is given by

$$P(\lambda) = \lambda^3 + c_1\lambda^2 + c_2\lambda + c_3,$$

$$\begin{aligned} c_1 &= m_{11} + m_{22} + m_{33}, \\ c_2 &= m_{12}m_{21} + m_{13}m_{31} - m_{32}a_{23} + m_{11}m_{22} + m_{11}m_{33} + m_{22}m_{33}, \\ c_3 &= m_{11}(m_{22}m_{33} - m_{32}a_{23}) + m_{21}(m_{12}m_{33} + m_{32}m_{13}) + m_{31}(m_{12}a_{23} + m_{13}m_{22}). \end{aligned}$$

According to Routh–Hurwitz criterion, E_1 is LES if and only if

$$c_1 > 0, \quad c_3 > 0 \quad \text{and} \quad c_4 = c_1c_2 - c_3 > 0. \tag{5}$$

We have the following results:

Lemme 2.2 *All m_{ij} are positive for all $i, j = 1, \ldots, 3$ with $(i, j) \neq (2, 3)$ and we have $c_1 > 0$.*

The next lemma shows that the sign of c_3 is given by the position of the curve of the function $H(\cdot)$ with respect to the line δ of equation $y = D(S_{in} - S)$ (see Fig. 3(b)). More precisely, we give the link between the determinant of the Jacobian matrix J_1 at $E_1 = (S^*, u^*, v^*)$ and $D + H'(S^*)$.

Proposition 2.4 *One has $c_3 = -\det(J_1) = -\varphi(S^*)(\psi(S^*) - b)(D + H'(S^*))$.*

Since the condition $c_4 > 0$ of the Routh–Hurwitz criterion (5) could be unfulfilled, we will study the behavior of flocculation model (1) according to the dilution rate and the disappearance rates of planktonic and attached bacteria. In fact, there exist four cases that must be distinguished:

$$\begin{array}{ll} \text{Case 1:} \quad D_u \leq D_v \leq D, & \text{Case 2:} \quad D_v < D_u \leq D, \\ \text{Case 3:} \quad D_v < D_u \text{ and } D < D_u, & \text{Case 4:} \quad D_u \leq D_v \text{ and } D < D_v. \end{array} \tag{6}$$

To determine the local stability of the positive steady state in the first and second cases of (6), we will have need of the following.

Proposition 2.5 *In the cases 1 and 2 ($D_u \leq D$ and $D_v \leq D$), we have $c_4 > 0$.*

It was shown in [8], see also [12, 13] that if $D_u = D_v = D$ then the positive steady E_1 exists and is unique and LES if and only if $S_{in} > \lambda_u$. Actually, this result holds in case 1.

Proposition 2.6 *In the case 1 ($D_u \leq D_v \leq D$), the positive steady state $E_1 = (S^*, u^*, v^*)$ exists if and only if $S_{in} > \lambda_u$. If it exists, it is unique and LES.*

The case 2 was solved in [3] where it was shown that the stability depends only on the relative position of the curve of function $y = H(S)$ and the straight line δ of equation $y = D(S_{in} - S)$ that is to say, on the sign of $D + H'(S^*)$. More precisely, we have:

Proposition 2.7 *Let $E_1 = (S^*, u^*, v^*)$ be a positive steady state. Assume that case 2 holds.*

1) If $\lambda_u < \lambda_v$: E_1 is LES if $H'(S^*) > -D$ and is unstable if $H'(S^*) < -D$.

2) If $\lambda_u > \lambda_v$: E_1 is LES if $H'(S^*) < -D$ and is unstable if $H'(S^*) > -D$.

In the case 3 of (6), when

$$D < D_v \leq D_u \quad \text{or} \quad D_v < D \leq D_u$$

c_4 can change sign by varying the control parameter S_{in} such that the positive steady state E_1 could change its behavior without any collision with another steady state [6]. In fact, numerical simulations show the emergence of stable limit cycles by Hopf bifurcations.

In case 4 of (6), we always have $\lambda_u < \lambda_v$ and $H'(S) > 0$. Therefore, from Prop. 2.4, it is deduced that in case 4 of (6) we always have $c_3 > 0$. We were not able to find a set of parameters for which $c_4 < 0$, as in the case 3 of (6) and we conjecture that in this case the positive steady state E_1 which is unique as soon as it exists, is also LES as soon as it exists.

3. Operating diagrams

The operating diagrams show how the system behaves when we vary the two control parameters S_{in} and D in (1). All other parameters in (1) are fixed, such as growth functions and specific attachment and detachment velocities. In fact, they depend on the nature of the organisms and the substrate introduced into the chemostat. Note that the operating diagrams of flocculation model (1) have not been studied in the existing literature in the generic case where the disappearance rates are distinct.

If $m_u \geq f(+\infty)$ then equation

$$f(S) = \alpha D + m_u \tag{7}$$

has no solution. We assume that $m_u < f(+\infty)$. The equation (7) is equivalent to

$$D = \widetilde{f}(S) := \frac{f(S) - m_u}{\alpha}.$$

Since f is increasing, then there exists a unique increasing function

$$\begin{array}{rccl} F_u : [0, & \overline{D}_u[& \longrightarrow & \left[f^{-1}(m_u), +\infty\right[\\ & D & \longrightarrow & F_u(D) = \widetilde{f}^{-1}(D) \end{array}$$

solution of equation (7) where

$$\overline{D}_u = \frac{f(+\infty) - m_u}{\alpha}.$$

Note that if $D \geq \overline{D}_u$, then equation (7) has no solution and we put $F_u(D) = +\infty$. If $m_v \geq g(+\infty)$ then equation

$$g(S) = \beta D + m_v \tag{8}$$

has no solution. We assume that $m_v < g(+\infty)$. The equation (8) is equivalent to

$$D = \widetilde{g}(S) := \frac{g(S) - m_v}{\beta}.$$

Since g is increasing, then there exists a unique increasing function

$$\begin{array}{rccl} F_v : [0, & \overline{D}_v[& \longrightarrow & \left[g^{-1}(m_v), +\infty\right[\\ & D & \longrightarrow & F_v(D) = \widetilde{g}^{-1}(D) \end{array}$$

solution of equation (8) where

$$\overline{D}_v = \frac{g(+\infty) - m_v}{\beta}.$$

Note that if $D \geq \overline{D}_v$, then equation (8) has no solution and we put $F_v(D) = +\infty$. If $m_v + b \geq g(+\infty)$ then equation

$$g(S) = \beta D + m_v + b \tag{9}$$

has no solution. We assume that $m_v + b < g(+\infty)$. The equation (9) is equivalent to

$$D = \widetilde{g}_b(S) := \frac{g(S) - m_v - b}{\beta}.$$

Since g is increasing, then there exists a unique increasing function

$$\begin{array}{rccl} F_b : [0, & \overline{D}_b[& \longrightarrow & \left[g^{-1}(m_v + b), +\infty\right[\\ & D & \longrightarrow & F_b(D) = \widetilde{g}_b^{-1}(D) \end{array}$$

solution of equation (9) where

$$\overline{D}_b = \frac{g(+\infty) - m_v - b}{\beta}.$$

Note that if $D \geq \overline{D}_b$, then equation (9) has no solution and we put $F_b(D) = +\infty$.

In the following, we show the emergence of the bi-stability region with multiplicity of positive steady states in the case

$$F_v(D) < F_u(D) < F_b(D) \quad \text{for all} \quad D \in \left[0, \min\left(\overline{D}_u, \overline{D}_v, \overline{D}_b\right)\right[.$$

In this case, the function H is defined and decreasing on the interval $I =]\lambda_v, \lambda_u[$ (See Lemma 2.5 of [6]). It vanishes at λ_u and tends to infinity as S tends to λ_v (see Fig. 3(b)). Assume that H is convex. Thus, equation $H'(S) = -D$ has a unique solution

$$\widetilde{S}(D) \in I =]\lambda_v, \lambda_u[\quad \text{if and only if} \quad H'(\lambda_u) + D > 0,$$

or also $D > \overline{D}$ with $\overline{D}$ solution of equation

$$H'(F_u(D)) + D = 0.$$

More precisely, since the function H' is increasing, then there exists a unique decreasing function

$$\begin{array}{rccl} \widetilde{S} : [\overline{D}, & \overline{D}_v[& \longrightarrow &]\lambda_v, \lambda_u[\\ & D & \longrightarrow & \widetilde{S}(D) = \widetilde{H}^{-1}(D) \end{array}$$

solution of equation $H'(S) = -D$ with $\widetilde{H}(S) = -H'(S)$. Thus, we define the curve Γ_{SN} of equation

$$S_{in} = F_{SN}(D) := \frac{1}{D} H(\widetilde{S}(D)) + \widetilde{S}(D)$$

which corresponds to the saddle-node bifurcation with the appearance of two positive steady states. In order to illustrate the operating diagram, we considered the parameter values provided in Table 2 with the growth rates f and g of Monod-type:

$$f(S) = \frac{m_1 S}{k_1 + S} \quad \text{and} \quad g(S) = \frac{m_2 S}{k_2 + S}, \tag{10}$$

where m_i denotes the maximum growth rate and k_i the Michaelis-Menten constant, $i = 1, 2$. Table 1 shows the existence and local stability of steady states E_0, E_1 and E_2 in the regions $\mathcal{I}_k$, $k = 0, 1, 2$, of the operating diagram shown in Fig. 1(b). The letter S (resp. U) means stable (resp. unstable). Absence of letter means that the corresponding steady state does not exist.

Table 1. *Existence and local stability of steady states according to the regions in the operating diagram of Fig. 1(b).*

Condition	Region	Color	E_0	E_1	E_2
$S_{in} < F_{SN}(D)$	$(D, S_{in}) \in \mathcal{I}_0$	cyan	S		
$F_{SN}(D) < S_{in} < F_u(D)$	$(D, S_{in}) \in \mathcal{I}_1$	green	S	S	I
$F_u(D) < S_{in}$	$(D, S_{in}) \in \mathcal{I}_2$	red	I	S	

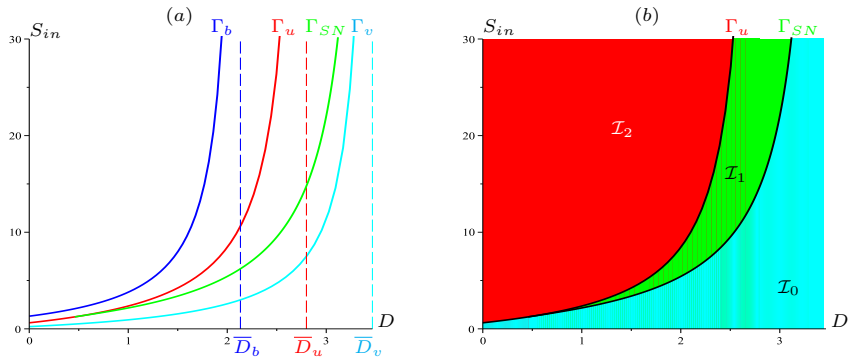

Figure 1. *Case $F_v(D) < F_u(D) < F_b(D)$: (a) the three curves Γ_v, Γ_u and Γ_b do not intersect and the curves Γ_u and Γ_{SN} intersect in $(D^*, S_{in}^*) = (0.46, 1.239)$. (b) The corresponding operating diagram of (1).*

Let Γ_i, $i = u, v, b, SN$, be the respective curves of equations $S_{in} = F_i(D)$ (see Fig. 1(a)). Γ_u and Γ_{SN} separate the operative plan (D, S_{in}) at most in three regions, denoted $\mathcal{I}_k$, $k = 0, 1, 2$ (see Fig. 1(b)). The transition from the region $\mathcal{I}_0$ to the region $\mathcal{I}_1$ by the curve Γ_{SN} (in green) corresponds to a saddle-node bifurcation with the appearance of two positive steady states E_1 which is LES and E_2 which is unstable. The transition from the region $\mathcal{I}_1$ to the region $\mathcal{I}_2$ by the curve Γ_u (in red) corresponds to a transcritical bifurcation when the unstable steady state E_2 disappears and E_0 becomes unstable.

For this set of parameters mentioned in Table 2, the numerical simulations show that the condition $c_4 > 0$ of the Routh–Hurwitz criterion is satisfied in the region $\mathcal{I}_1$, that is, the steady state E_1 is LES as long as it exists. However, this condition may not be satisfied for another set of parameters where the positive steady state can change behavior

by a Hopf bifurcation with the emergence of a stable limit cycle. In this case, the analysis of the operating diagram is the subject of on-going investigations.

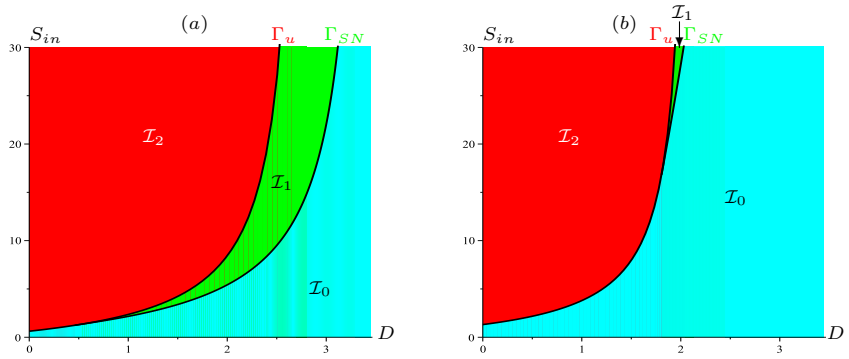

Figure 2. *Effect of mortality on the operating diagram: (a)* $m_u = 0.7$ *(b)* $m_u = 50$.

Fig. 2 shows the reduction of the bi-stability region (in green) $\mathcal{I}_1$ and the coexistence region (in red) $\mathcal{I}_2$ by increasing the value of the mortality parameter of the isolated bacteria while the washout region (in cyan) $\mathcal{I}_0$ increases. Hence, the importance of mortality on the behavior of the system and the destabilization of the microbial ecosystem and the maintenance of the least competitive species and hence coexistence. Thus, the control parameter values should be chosen in the region $\mathcal{I}_2$ in order to protect the coexistence of two microbial species in this process. However, an appropriate initial condition should be chosen to achieve a good operation of the process when the operating parameters are in the region $\mathcal{I}_1$.

4. The one-parameter bifurcation diagrams and numerical simulations

Our aim in this section is to study the behavior of system (1) when the parameter S_{in} is varying and all other parameters are fixed. In order to validate the theoretical results of the operating diagram, the diamond point $(D^*, S_{in}^*) = (2, 6)$ is chosen in the bi-stability region $\mathcal{I}_1$ where the existence and stability of the steady states are illustrated in Fig. 3. In fact, the positive steady states

$$E_1 \simeq (3.5, 0.583, 1.699) \quad \text{and} \quad E_2 \simeq (5.621, 0.198, 0.117)$$

are given by the intersection of the line δ of equation $y = D^*(S_{in}^* - S)$ and the curve of the function $H(\cdot)$. In all figures, we have chosen the red color for LES steady states and blue color for unstable steady states. From Prop. 2.4, $c_3(S^*) > 0$ since $\varphi(S^*) < 0$, $\psi(S^*) - b < 0$ and $H'(S^*) < -D$ in this case

$$\lambda_v \simeq 2.591 < \lambda_u \simeq 8.437 < \lambda_b = 43.5.$$

Moreover, Fig. 3(b) shows that $c_4(S^*) > 0$ for all $S^* \in I$ defined by (4). Using Lemma 2.2, it follows that all the conditions of the Routh-Hurwitz criterion are satisfied, that is,

E_1 is LES as long as it exists. Note that the curve of the function $H(\cdot)$ is tangent to the line δ of equation $y = D^*(S_{in}^{SN} - S)$ in $\widetilde{S} \simeq 4.338$ such that

$$S_{in}^{SN} = \frac{1}{D} H(\widetilde{S}) + \widetilde{S} \simeq 5.426.$$

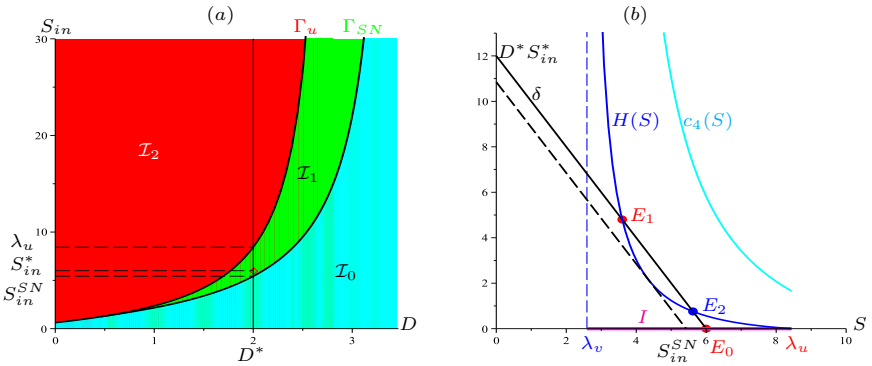

Figure 3. *(a) The operating diagram of (1) when $F_v(D) < F_u(D) < F_b(D)$. (b) The corresponding existence and stability of steady states when the diamond point $(D^*, S_{in}^*) = (2, 6) \in \mathcal{I}_1$.*

Fig. 4(a) shows the coexistence between the two species for an initial condition

$$S(0) = S^{**} + \varepsilon, \quad u(0) = u^{**} + \varepsilon, \quad v(0) = u^{**} + \varepsilon,$$

where $\varepsilon = 10^{-3}$ and

$$E_2 = (S^{**}, u^{**}, v^{**}) \simeq (5.621, 0.198, 0.117).$$

The solution of model (1) converges toward the coexistence steady state E_1 which is LES. Fig. 4(b) shows the extinction of two species for an initial condition

$$S(0) = S^{**} - \varepsilon, \quad u(0) = u^{**} - \varepsilon, \quad v(0) = u^{**} - \varepsilon.$$

and the convergence toward the washout steady state $E_0 = (6, 0, 0)$ which is LES.

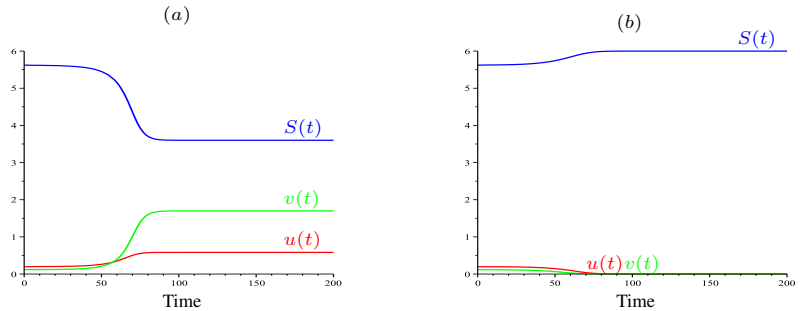

Figure 4. *The system exhibits a bi-stability: according to the initial condition, there is either (a) coexistence of the two species (convergence toward E_1) or (b) washout of the two species (convergence toward E_0).*

Fig. 5 illustrates the trajectories over time in three-dimensional space (S, u, v) for several positive initial conditions. For $(D^*, S_{in}^*) = (2, 6) \in \mathcal{I}_1$, Fig. 5(a) shows the bi-stability with two basins of attraction, one toward the washout steady state E_0 and the other toward the coexistence steady state E_1 which are stable nodes. These two basins are separated by the stable manifold of saddle point E_2. For $(D^*, S_{in}^*) = (2, 9) \in \mathcal{I}_2$, the numerical simulations can show the global convergence toward the positive steady state $E_1 = (3.07, 0.77, 5.15)$ from any positive initial condition (see Fig. 5(b)).

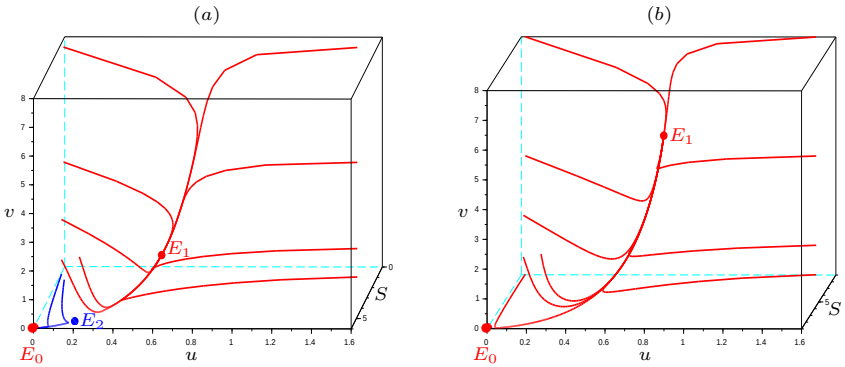

Figure 5. *The trajectories of system (1) in three-dimensional space* (S, u, v) *(a) the bi-stability of* E_0 *and* E_1 *when* $(D^*, S_{in}^*) = (2, 6) \in \mathcal{I}_1$. *(b) Global convergence to* E_1 *when* $(D^*, S_{in}^*) = (2, 9) \in \mathcal{I}_2$.

Finally, we study the one-parameter bifurcation diagram for system (1) as the control parameter S_{in} varies while D is fixed ($D = D^* = 2$). Fig. 6 shows a saddle-node bifurcation between E_1 and E_2 at the cyan circle point for $S_{in} = S_{in}^{SN} \simeq 5.426$. Then, the washout steady state E_0 loses its stability by a transcritical bifurcation with E_2 at the green diamond point for $S_{in} = \lambda_u \simeq 8.437$.

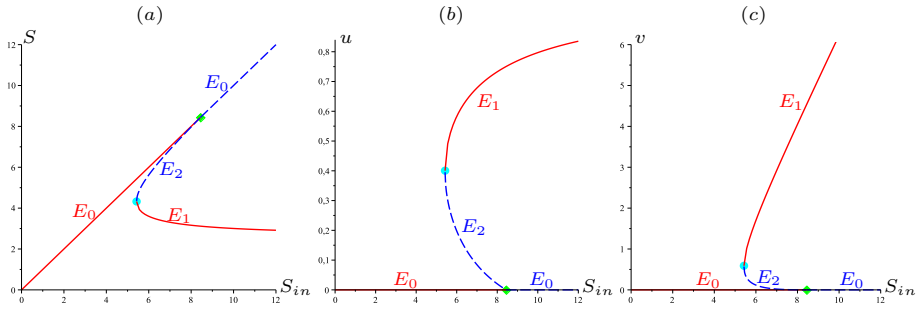

Figure 6. *One-parameter bifurcation diagrams for fixed* $D = 2$ *showing the effect on the components* S, u *and* v *of all steady states as* S_{in} *varies. Blue dashed curves corresponds to unstable steady states and red solid curves to the stable steady states. The green solid diamonds represent the transcritical bifurcations of* E_0 *and* E_2 *while the cyan solid circles represent the saddle-node bifurcations of* E_1 *and* E_2.

5. Conclusion

In this work, we have analyzed mathematically and through numerical simulations a model of the chemostat where one species is present in two forms, isolated and attached with the presence of a single resource. The new feature was that maintenance terms are added to removal rates in order to give a complete analysis of the flocculation model (1). The operating diagram shows the occurrence of the bi-stability region with multiplicity of coexistence steady states that can bifurcate through saddle-node bifurcations or transcritical bifurcations. However, the bi-stability could occur in the classic chemostat model [15] only when the growth rate is non-monotonic. Furthermore, the operating diagrams show the effect of mortality of the planktonic bacteria on the reduction of the bi-stability and the coexistence regions by promoting the washout of the species and the destabilization of the microbial ecosystem. Finally, the one-parameter bifurcation diagram shows the effect of the control parameter S_{in} on the behavior of the system.

Acknowledgments. The first author thanks the LAMSIN (LR-99-ES20), ENIT, University of Tunis El Manar and the French national research institute INRIA for their financial support to participate to CARI 2018 at Stellenbosch University in South Africa, where part of this work was presented. The authors thank the Euro-Mediterranean research network TREASURE (`http://www.inra.fr/treasure`).

A. Parameters used in numerical simulations

Table 2. *Parameter values used for (1) when the growth rates f and g are given by (10).*

Parameter	m_1 (h^{-1})	k_1 (g/l)	m_2 (h^{-1})	k_2 (g/l)	a $(l/h/g)$	b (h^{-1})	α	β	m_u (h^{-1})	m_v (h^{-1})
Figs. 1, 3, 4, 5, 6	3.5	2.5	3	1.5	1	1	1	0.75	0.7	0.4
Fig. 2									50	

B. References

[1] B. BENYAHIA, T. SARI, B. CHERKI, J. HARMAND, "Bifurcation and stability analysis of a two step model for monitoring anaerobic digestion processes", *J. Process Control*, vol. 22, 2012, 1008–1019.

[2] O. BERNARD, Z. HADJ-SADOK, D. DOCHAIN, A. GENOVESI, J-P. STEYER, "Dynamical model development and parameter identification for an anaerobic wastewater treatment process", *Biotechnol. Bioeng.*, vol. 75, 2001, 424–438.

[3] R. FEKIH-SALEM, "Modèles mathématiques pour la compétition et la coexistence des espèces microbiennes dans un chémostat", *PhD thesis, UM2-UTM*, 2013.

[4] R. FEKIH-SALEM, J. HARMAND, C. LOBRY, A. RAPAPORT, T. SARI, "Extensions of the chemostat model with flocculation", *J. Math. Anal. Appl.*, vol. 397, 2013, 292–306.

[5] R. FEKIH-SALEM, A. RAPAPORT, T. SARI, "Emergence of coexistence and limit cycles in the chemostat model with flocculation for a general class of functional responses", *Appl. Math.*

Modell., vol. 40, 2016, 7656–7677.

[6] R. FEKIH-SALEM, T. SARI, "Properties of the chemostat model with aggregated biomass and distinct removal rates", *SIAM J. Appl. Dyn. Syst.*, vol. 18, 2019, 481–509.

[7] R. FRETER, H. BRICKNER, S. TEMME, "An understanding of colonization resistance of the mammalian large intestine requires mathematical analysis", *Microecology and Therapy*, vol. 16, 1986, 147–155.

[8] J. HARMAND, C. LOBRY, A. RAPAPORT, T. SARI, "The Chemostat: Mathematical Theory of Microorganism Cultures", *Chemical Eng. Ser., Chemostat Bioprocesses Set, Wiley, New York*, 2017.

[9] B. HAEGEMAN, A. RAPAPORT, "How flocculation can explain coexistence in the chemostat", *J. Biol. Dyn.*, vol. 2, 2008, 1–13.

[10] IWA TASK GROUP ON BIOFILM MODELING, "Mathematical modeling of biofilms", *IWA publishing*, 2006.

[11] S. MARSILI-LIBELLI, S. BENI, "Shock load modelling in the anaerobic digestion process", *Ecol. Model.*, vol. 84, 1996, 215–232.

[12] A. RAPAPORT, "Properties of the chemostat model with aggregated biomass", *Eur. J. Appl. Math.*, vol. 29, 2018, 972–990.

[13] T. SARI, R. FEKIH-SALEM, "Analysis of a model of flocculation in the chemostat", *Proceedings of the 8th conference on Trends in Applied Mathematics in Tunisia, Algeria, Morocco*, 2017, 75–80.

[14] S. SHEN, G. C. PREMIER, A. GUWY, R. DINSDALE, "Bifurcation and stability analysis of an anaerobic digestion model", *Nonlinear Dyn.*, vol. 48, 2007, 391–408.

[15] H.L. SMITH, P. WALTMAN, "The Theory of the Chemostat: Dynamics of Microbial Competition", *Cambridge University Press, Cambridge, UK*, 1995.

[16] D.N. THOMAS, S.J. JUDD, N. FAWCETT, "Flocculation modelling: a review", *Water Res.*, vol. 33, 1999, 1579–1592.